Journal of Sound and Vibration (2001) **245**(1), 151–164
doi:10.1006/jsvi.2001.3559, available online at http://www.idealibrary.com on IDEAL®

DYNAMIC ANALYSIS OF A SELF-EXCITED HYSTERETIC SYSTEM

Q. DING

School of Mechanical Engineering, Tianjin University, 300072 *Tianjin, People's Republic of China*

AND

A. Y. T. LEUNG† AND J. E. COOPER

*School of Engineering, University of Manchester, Manchester M*13 9*PL, England.*
E-mail: andrew.leung@cityu.edu.hk

(*Received* 10 *May* 2000, *and in final form* 4 *January* 2001)

The dynamic behaviour of a self-excited system with hysteretic non-linearity is investigated in this paper. The averaging method is applied to the autonomous system and the resulting bifurcation equation of the self-excited response is analyzed using the singularity theory. The study of the bifurcation diagrams reveals the multivalued and jumping phenomena due to the effect of the hysteretic non-linearity. Secondly, the steady state response of the averaged system of the non-autonomous oscillator in primary resonance is investigated. Due to the effect of the hysteretic non-linearity, the system exhibits softening spring behaviour. A stability analysis shows that the steady state periodic response exists over a limited excitation frequency range. It loses its stability outside the frequency range through Hopf bifurcation and then the system undergoes quasi-periodic motion. Finally, by using circle maps to get winding numbers, various orders of super- and subharmonic resonance and mode-locking are investigated. The mode-locking, alternating with the quasi-periodic responses, takes place according to the Farey number tree as revealed in many other systems. The increase of the hystereticity can improve the stability of subharmonic resonance.

1. INTRODUCTION

Many structures are constructed in such a manner that a limited amount of slip takes place between members either by tolerance design or as a consequence of deterioration. This is particularly true for structures of a riveted or bolted construction. The restoring mechanism of such a case can be considered as a hysteretic damper, as illustrated by Neyfeh and Mook [1]. Hysteretic systems are non-smooth. Methods that are useful in smooth dynamical systems are not applicable in this case. These include the Lyapunov–Schmidt reduction, the centre manifold procedure and the normal form method [2, 3]. Nevertheless, classical methods in non-linear oscillation, such as the averaging method, are particularly useful for the analytical investigation of the dynamic behaviour of the hysteretic systems. The averaging method was shown to be equivalent to the normal form method [4]. Using the averaging method, Iwan and Furuike [5] studied the effect of hysteretic non-linearity on the

†Present address: Department of Building and Construction, City University of Hong Kong, Kowloon, Hong Kong.

0022-460X/01/310151 + 14 $35.00/0

transient and steady state responses of a single-degree-of-freedom dynamical system. The results showed that a first order approximate analysis is quite adequate for this system.

Self-excited vibrations occur in many physical systems, such as supersonic flutter of plates and shells [6], whirl/whip instabilities of rotor/bearing systems [7] and rotor/seal systems [8], and an *van der Pol* oscillator in an electrical circuit [1]. The cause is either a negative damping or cross-stiffness (sources of cross-coupling in two transverse directions of the displacement space). Usually when a critical value is exceeded by a critical parameter, the system motion changes to a mode that is not conformable to external forces, and may be extremely dependent on the initial conditions in some cases. This transition of the motion pattern is called Hopf bifurcation and the resulting bounded motion is referred to as a limit circle. A simple typical model of the self-excited system is described by the van der Pol equation that has been extensively used in studying many self-excited phenomena [1].

Further, self-excited systems with hysteretic non-linearity abound in engineering. These include an airfoil with hysteretic non-linearity when in supersonic flutter [6]. However, studies on the non-linear dynamic behaviour of a self-excited system with hysteretic non-linearity, to the authors' knowledge, are rarely reported. In this paper, the averaging method is applied to a van der Pol system to obtain the averaged equations. For an autonomous system, the bifurcation of the averaged equation is analyzed using singularity theory to get the transition sets in the hysteretic parameter plane. For a non-autonomous system, the steady state response in primary resonance is investigated and the stability analyses of the response are provided to show the occurrence of quasi-periodic motion. Using circle maps to get winding numbers, the phenomenon of mode-locking alternating with quasi-periodic responses, over the frequency range of the external excitation from before to after the primary resonance, is also revealed.

2. EQUATION OF MOTION

Consider the system in Figure 1. The mass is attached to a linear elastic spring, negative damping (van der Pol type) and a hysteretic damper. The hysteretic damper consists of a linear elastic spring and a Coulomb damper with amplitude constraint in two directions. The hardening-type hysteretic restoring force $F(x)$ is shown in Figure 2 in which x represents the displacement of the mass. The relationships can be described by lines I–VII and are tabulated in Table 1. For periodic responses, the travelling path depends on the level of x_{amp}, the amplitude of x, as indicated in Table 2. The system is in a sliding stage for $x_{amp} \in [a, a + b]$, because the Coulomb damper is sliding when the mass changes its direction of motion. Rationally, it is in a constraint stage for $x_{amp} > a + b$ because sliding is already stopped by the amplitude constraint when the mass changes its direction of motion.

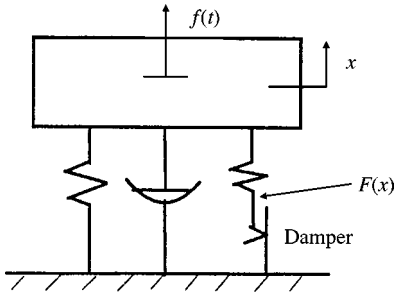

Figure 1. A self-sustained system with hysteretic non-linearity.

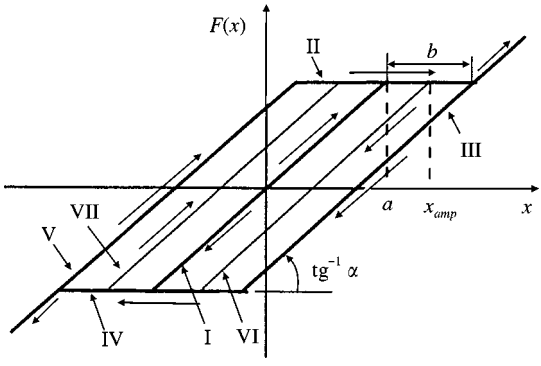

Figure 2. The hysteresis restoring force with a hysteretic damper.

TABLE 1

The relationship of $F(x)$ with x

Line	x	$F(x)$
I	(a, a)	αx
II	$[a-b, a+b)$	αa
III	$(b-a, +\infty)$	$\alpha(x-b)$
IV	$(-a-b, b-a]$	$-\alpha a$
V	$(-\infty, a-b)$	$\alpha(x+b)$
VI	$(x_{amp}-2a, x_{amp})$	$\alpha(x+a-x_{amp})$
VII	$(-x_{amp}, 2a-x_{amp})$	$\alpha(x-a+x_{amp})$

TABLE 2

Travelling path of $F(x)-x$

x_{amp}	$F(x)$
$(0, a)$	I
$[a, a+b]$	II → VI → IV → VII → II
$(a+b, \infty)$	II → III → III → IV → V → V → II

Besides the periodic response, the mass can also change its direction of motion irregularly. In all cases, $F(x)$ will travel along a slope line after the occurrence of the change of the directions of motion either the same one along which the mass is travelling, or a new one across the point in a horizontal line.

The dimensionless equation of motion of the system can be written as

$$\ddot{x} + x - (\beta - x^2)\dot{x} + F(x) = f(t), \tag{1}$$

where $f(t) = K\cos\Omega t$ is an external force acting on the mass and β is the coefficient of the van der Pol damping. It is well known that for the autonomous van der Pol system, Hopf bifurcation occurs at $\beta = 0$ and the system will undergo self-excited vibration as β increases [9]. So β is taken as the bifurcation parameter in section 3.

3. BIFURCATION OF THE AUTONOMOUS SYSTEM

3.1. AVERAGING

For an autonomous self-excited system with hysteretic non-linearity, $K = 0$. With a small positive parameter ε equation (1) can be rewritten in the following form that is suitable for averaging:

$$\ddot{x} + x = \varepsilon[(\beta - x^2)\dot{x} - F(x)]. \tag{2}$$

Transforming the dependent variable from x to u and θ where

$$x = u\cos\psi, \qquad \dot{x} = -u\sin\psi, \qquad \psi = t + \theta$$

gives the standard form of the equation governing u and θ:

$$\frac{\mathrm{d}u}{\mathrm{d}t} = \varepsilon[u(\beta - u^2\cos^2\psi)\sin^2\psi + F(u\cos\psi)\sin\psi],$$

$$\frac{\mathrm{d}\theta}{\mathrm{d}t} = \varepsilon\left[(\beta - u^2\cos^2\psi)\sin\psi\cos\psi + \frac{1}{u}F(u\cos\psi)\cos\psi\right]. \tag{3}$$

Using the Krylov–Bogoliubov first order approximation,

$$\begin{aligned} u &= y + \varepsilon U(t, y, \gamma) + O(\varepsilon^2), \\ \theta &= \gamma + \varepsilon V(t, y, \gamma) + O(\varepsilon^2), \end{aligned} \tag{4}$$

where y and γ represent the amplitude and phase of the first order approximate solution of the system. The right-hand sides of equation (3) are averaged over ψ from 0 to 2π (assuming that y and γ are constants) to give

$$\frac{\mathrm{d}y}{\mathrm{d}t} = \frac{y}{2}[\beta - \tfrac{1}{4}y^2] + A(y),$$

$$\frac{\mathrm{d}\gamma}{\mathrm{d}t} = \frac{1}{y}B(y), \tag{5}$$

where

$$\mathrm{A}(y) = \frac{1}{2\pi}\int_0^{2\pi} F(y\cos\psi)\sin\psi\,\mathrm{d}\psi, \qquad B(y) = \frac{1}{2\pi}\int_0^{2\pi} F(y\cos\psi)\cos\psi\,\mathrm{d}\psi.$$

To perform the above integrations, let $\psi = 2\pi - \varphi$, then

$$\mathrm{A}(y) = -\frac{1}{2\pi}\int_0^{2\pi} F(y\cos\varphi)\sin\varphi\,\mathrm{d}\varphi, \qquad B(y) = \frac{1}{2\pi}\int_0^{2\pi} F(y\cos\varphi)\cos\varphi\,\mathrm{d}\varphi,$$

TABLE 3

Different expressions of $F(y\cos\varphi)$ and results of the integrals of $A(y)$ and $B(y)$

y	$F(y\cos\varphi)$		$A(y)$	$B(y)$
$(0, a)$	$\alpha y\cos\varphi$	$0 \leqslant \varphi \leqslant \pi$	0	$\frac{ay}{2}$
$[a, b+a]$	αa	$0 \leqslant \varphi \leqslant \varphi_3$	$-\frac{2\alpha a(y-a)}{\pi y}$	$\frac{\alpha y}{4\pi}[2(\pi-\varphi_3)+\sin 2\varphi_3]$
	$\alpha(y\cos\varphi + y - a)$	$\varphi_3 \leqslant \varphi \leqslant \pi$		
$(b+a, \infty]$	$\alpha(y\cos\varphi - b)$	$0 \leqslant \varphi \leqslant \varphi_1$	$-\frac{2ab\alpha}{\pi y}$	$\frac{\alpha y}{4\pi}[2(\pi+\varphi_1-\varphi_2)$
	αa	$\varphi_1 \leqslant \varphi \leqslant \varphi_2$		$+\sin 2\varphi_2 - \sin 2\varphi_1]$
	$\alpha(y\cos\varphi + b$	$\varphi_2 \leqslant \varphi \leqslant \pi$		

where φ represents an angle measured from axis x anti-clockwise in Figure 2. Define φ_1, φ_2 and φ_3 as

$$\varphi_1 = \cos^{-1}\left[\frac{a+b}{y}\right], \qquad \varphi_2 = \cos^{-1}\left[\frac{a-b}{y}\right], \qquad \varphi_3 = \cos^{-1}\left[\frac{2a}{y} - 1\right]$$

and consider the symmetry of the hysteretic restoring force $F(x)$ over the range $[0, \pi]$. Corresponding to Tables 1 and 2, $F(y\cos\varphi)$ and the integrals of $A(y)$ and $B(y)$ are calculated and listed in Table 3 for different levels of the amplitude.

3.2. BIFURCATION ANALYSIS

The steady state responses of the averaged system (5), which are actually the bifurcation equations, can be obtained by setting $\mathrm{d}y/\mathrm{d}t = \mathrm{d}\gamma/\mathrm{d}t = 0$, to yield

$$Y_1(y, \lambda, \kappa) = y(y^2 - \lambda) = 0, \quad y < a, \tag{6a}$$

$$Y_2(y, \lambda, \kappa) = y^4 - \lambda y^2 + \kappa_1 y + \kappa_2 = 0, \quad a < y < a + b, \tag{6b}$$

$$Y_3(y, \lambda, \kappa) = y^4 - \lambda y^2 + \kappa_3 = 0, \quad y > a + b, \tag{6c}$$

where $\lambda = 4\beta$, $\kappa_1 = 16\alpha a/\pi$, $\kappa_2 = -a\kappa_1$, $\kappa_3 = b\kappa_1$. Taking λ as a bifurcation parameter and κ as an unfolding parameter space, the bifurcation set **B**s and the hysterestic set **H**s for the bifurcation equations $Y_2 = 0$ and $Y_3 = 0$ on plane (α, a) can be calculated according to the method of singularity [10]. The results are listed in Table 4 (the double limit sets **DL**s are empty). Due to the discontinuity of the connecting points of equations (6), the connecting set $\mathbf{TL}_2$ for $Y_2 = 0$ and $Y_3 = 0$ are also calculated (whilst $\mathbf{TL}_1$ for $Y_1 = 0$ and $Y_2 = 0$ is empty).

Therefore, the transition sets $\mathbf{\Sigma} = \mathbf{B} \cup \mathbf{H} \cup \underline{\mathbf{B}} \cup \mathbf{TL}_2$ (**B** and **H** belong to $Y_2 = 0$, whilst $\underline{\mathbf{B}}$ belongs to $Y_3 = 0$) are found in Figure 3(a). The plane (α, a) for $a > 0$ and $\alpha > 0$ is divided

TABLE 4

Transition sets of bifurcation equation (6)

Bifurcation equation	**B**	**H**	**TL$_2$**
$Y_2(y, \lambda, \kappa) = 0$	$\{\alpha = 0 \text{ or } a = 0\}$	$\left\{\alpha = 0 \text{ or } a = 0 \text{ or } a^2 = \frac{27\alpha}{256\pi}\right\}$	$\left\{(a+b)^4 = \frac{16b\alpha}{\pi} a\right\}$
$Y_3(y, \lambda, \kappa) = 0$	$\{\alpha = 0 \text{ or } a = 0\}$	Φ(empty)	

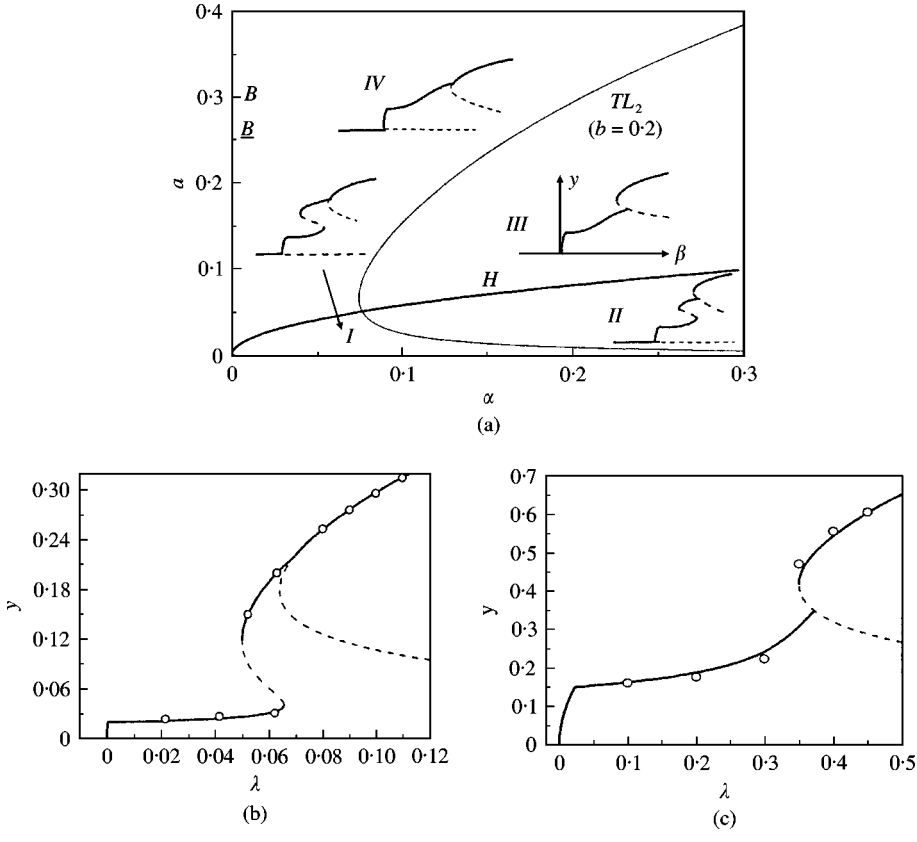

Figure 3. (a) Transition sets of averaged system (5). (b) and (c) Steady state responses of system (2) in parameter areas I and III: - - - - -, theoritical value; ○, numerical value.

into four areas and the bifurcation diagrams are persistent, or topologically equivalent in every area. The theoretically predicted results in the four areas and the corresponding simulated results can be obtained by solving equation (6) and the original system (1), respectively. The results for areas I and III in Figure 3(b) and (c) show that the analysis based on the first order approximate averaging method is quite accurate for the autonomous self-excited system with hysteretic non-linearity.

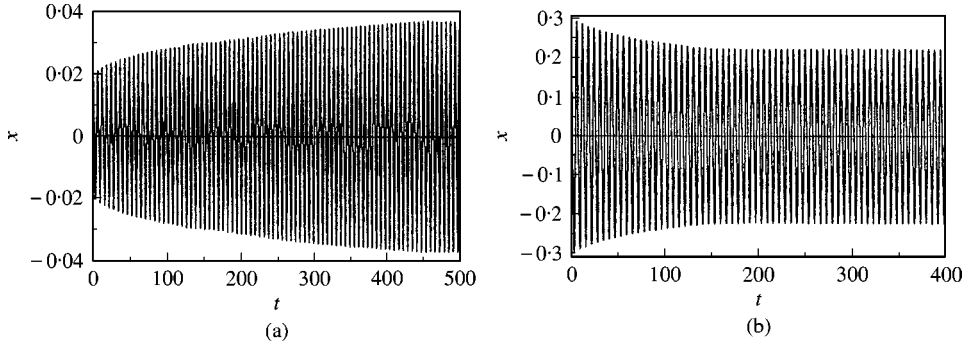

Figure 4. Initial conditions determine which of the multivalued responses is actual ($\alpha = 0{\cdot}05$, $a = 0{\cdot}02$, $b = 0{\cdot}2$, $\lambda = 0{\cdot}06$): (a) small amplitude vibration (initial values: 0·02, 0); (b) large amplitude vibration (initial values: 0·3, 0).

The steady state self-excited response of the van der Pol system is described by equation 6(a) for any value of amplitude y. Due to the introduction of the hysteretic non-linearity, the response of the system should be described by equations 6(a)–(c). The multivalues and jump phenomena revealed in Figure 3 occur for $y \in [a, a + b]$, when the system is in the sliding stage, under certain values of parameters a, α and β. When two stable steady state solutions exist simultaneously, the initial conditions determine which of these represents the actual response of the system. Letting the values of the parameters to be the same as in Figure 3(b) and selecting $\lambda = 0{\cdot}06$ which corresponds to two stable steady state solutions, the small-amplitude vibration and the large-amplitude vibration for different initial conditions, respectively, are obtained as shown in Figure 4.

4. PRIMARY RESONANCE OF THE NON-AUTONOMOUS SYSTEM

4.1. AVERAGING

To analyze the response of the non-autonomous system (1) in primary resonance, that is $\Omega \approx 1$. $K = \varepsilon k$. Then equation (1) can be rewritten as

$$\ddot{x} + x = \varepsilon[(\beta - x^2)\dot{x} - F(x) + k\cos\Omega t]. \tag{7}$$

Transforming the dependent variable from x to u and θ where

$$x = u\cos\psi, \qquad \dot{x} = -u\sin\psi, \qquad \psi = \Omega t + \theta$$

gives the following standard form of the equation governing u and θ:

$$\begin{aligned} \frac{\mathrm{d}u}{\mathrm{d}t} &= \varepsilon[(\beta - u^2\cos^2\psi)u\sin\psi + F(u\cos\psi) - k\cos\Omega t]\sin\psi, \\ \frac{\mathrm{d}\theta}{\mathrm{d}t} &= 1 - \Omega + \frac{\varepsilon}{u}[(\beta - u^2\cos^2\psi)\sin\psi + F(u\cos\psi) - k\cos\Omega t]\cos\psi. \end{aligned} \tag{8}$$

Using the procedure similar to that in section 3, the first order approximate averaging equations are

$$\frac{\mathrm{d}y}{\mathrm{d}t} = \frac{y}{2}\left[\beta - \frac{1}{4}y^2\right] + A(y) - \frac{k}{1+\Omega}\sin\gamma,$$
$$\frac{\mathrm{d}\gamma}{\mathrm{d}t} = 1 - \Omega + \frac{B(y)}{y} - \frac{k}{1+\Omega}\cos\gamma, \tag{9}$$

where $A(y)$ and $B(y)$ are listed in Table 3. The steady state response of equation (9) can be obtained from equations (10):

$$\Omega\left(\beta - \frac{1}{4}y^2\right) + 2\frac{A(y)}{y} = \frac{k}{y}\sin\gamma,$$
$$1 - \Omega^2 + 2\frac{B(y)}{y} = \frac{k}{y}\cos\gamma. \tag{10}$$

Squaring and adding the results of these equations gives

$$\left[\Omega\left(\beta - \frac{1}{4}y^2\right) + 2\frac{A(y)}{y}\right]^2 + \left(1 - \Omega^2 + 2\frac{B(y)}{y}\right)^2 = \left(\frac{k}{y}\right)^2. \tag{11}$$

Equation (11) is an implicit equation for the amplitude of the steady response y as a function of Ω and k, the frequency and the amplitude of the external excitation; β, the bifurcation parameter of the van der Pol system; and a, b and α, the hysteresis parameters. With the values of the system parameters, $a = 0{\cdot}3$, $b = 0{\cdot}8$, $\alpha = 1$ and $\beta = 0{\cdot}5$ and 1 respectively the estimated frequency–amplitude curves are shown in Figure 5. For weak excitation, when the level of excitation is less than a critical value k_c, the response diagrams consist of two disconnected branches—a lower branch running near the Ω-axis and an upper branch consisting of a closed curve (see for example, $\beta = 0{\cdot}5$, $k = 0{\cdot}1$ and $\beta = 1$, $k = 0{\cdot}3$ and $0{\cdot}5$). When k tends to be zero, the upper ones tend to be a point. Following the calculation, the degenerating points can be located at (1·14, 1·03) and (1·25, 1·91) for $\beta = 0{\cdot}5$ and 1 respectively. Contrarily, as k increases, the upper curves expand while the lower ones move away from the Ω-axis. For sufficiently large k, say $k \geqslant k_c$, the two branches join together ($\beta = 0{\cdot}5$, $k_c = 0{\cdot}175$; $\beta = 1$, $k_c = 0{\cdot}81$). It is obvious that the amplitude of the resonant response increases with k, other parameters being fixed. Similarly, it increases also with β when other parameters (including k) are fixed. For example, the maximum of y corresponding to $\beta = 0{\cdot}5$ and 1 is 1·58 and 2·21 for $k = 0{\cdot}5$, and 1·83 and 2·25 for $k = 1$ respectively.

In Figure 5, both $y = a$ (0·3) and $y = a + b$ (1·1) are represented by the dashed horizontal lines. For $y < a$ or $y > a + b$, the backbone curves (also dashed) bend to the right, so that the vibration of the system in primary resonance exhibits hardening spring behaviour. Otherwise, softening spring behaviour is exhibited and the backbone curve bends to the left. In general, the stiffness of the system decreases when it is in the sliding stage. As a result, the non-linear resonant frequency of the system can increase or decrease as Ω is increased. This characteristic results also from the hysteretic non-linearity in the system.

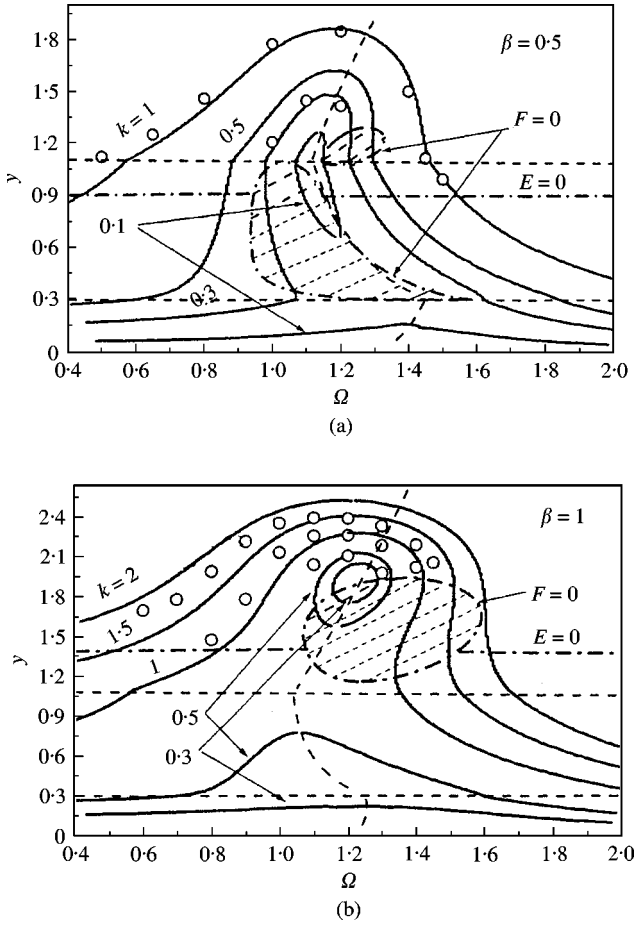

Figure 5. Frequency–amplitude curves ($a = 0{\cdot}3$, $b = 0{\cdot}8$, $\alpha = 1$): (a) $\beta = 0{\cdot}5$ (b) $\beta = 1$: ○—numerically stable solutions.

4.2. STABILITY ANALYSIS

In order to determine the stability of these steady state responses, let

$$y = y_s + y_p, \qquad \gamma = \gamma_s + \gamma_p, \tag{12}$$

where (y_s, γ_s) are the solutions of equations (10). y_p and γ_p represent the perturbations to the steady response. Substituting equation (12) into equation (9) and using equation (10), the linear terms are

$$\begin{aligned} \dot{y}_p &= \frac{1}{2}\left[\beta - \frac{3}{4}y_s^2 + A'(y_s)\right] y_p - \frac{k}{1+\Omega}\cos\gamma_s \gamma_p, \\ \dot{\gamma}_p &= \frac{1}{y_s}\left[B'(y_s) - \frac{B(y_s)}{y_s} + \frac{k}{1+\Omega}\frac{\cos\gamma_s}{y_s}\right] y_p + \frac{k}{1+\Omega}\frac{\sin\gamma_s}{y_s}\gamma_p, \end{aligned} \tag{13}$$

where

$$A'(y_s) = \left.\frac{\partial A(y)}{\partial y}\right|_{y=y_s}, \qquad B'(y_s) = \left.\frac{\partial B(y)}{\partial y}\right|_{y=y_s}.$$

Letting $y_p = \bar{y}_p e^{\lambda t}$ and $\gamma_p = \bar{\gamma}_p e^{\lambda t}$, one gets

$$\begin{aligned} &\frac{1}{2}\left[\beta - \frac{3}{4}y_s^2 + A'(y_s) - 2\lambda\right]\bar{y}_p - \frac{k}{1+\Omega}\cos\gamma_s\bar{\gamma}_p = 0, \\ &\frac{1}{y_s}\left[B'(y_s) - \frac{B(y_s)}{y_s} + \frac{k}{1+\Omega}\frac{\cos\gamma_s}{y_s}\right]\bar{y}_p + \left(\frac{k}{1+\Omega}\frac{\sin\gamma_s}{y_s} - \lambda\right)\bar{\gamma}_p = 0. \end{aligned} \tag{14}$$

Using equation (10), the characteristic polynomial of the non-trivial steady solution is

$$\lambda^2 - E\lambda + F = 0, \tag{15}$$

where

$$E = \beta - \frac{1}{2}y_s^2 + \frac{1}{2}A'(y_s) + \frac{A(y_s)}{y_s},$$

$$F = \frac{1}{4}\left[\beta - \frac{3}{4}y_s^2 + A'(y_s)\right]\left[\beta - \frac{1}{4}y_s^2 + 2\frac{A(y_s)}{y_s}\right] + [1 - \Omega + B'(y_s)]\left[1 - \Omega + \frac{B(y_s)}{y_s}\right].$$

When $F > 0$ and $E < 0$, the roots of equation (15) are real and negative, so the steady solutions are stable. When $F > 0$ and $E = 0$, there is a pair of pure imaginary eigenvalues for the averaged system (9), so Hopf bifurcation occurs. In this case, the motion of the original system (7) will be amplitude-modulated or quasi-periodic due to the two incommensurate frequencies involved in the motion; one is the frequency f of the external force and another the non-linear resonant frequency f_{cr} resulting from Hopf bifurcations. When $F < 0$, the roots of equation (15) are real with opposite signs, so the predicted motions correspond to saddle points and are unrealizable. Therefore, the stability of the steady state motion on the amplitude–frequency plane can be classified by the areas composed of the dash-pot curves $E = 0$ and $F = 0$, as indicated in Figure 5. The solutions located inside the enclosed shadow areas which represent $F < 0$ are unrealizable. From $E = 0$, a straight line parallel to Ω-axis, $y = y_E$, is obtained and $y > y_E$ results in $E < 0$. Therefore, the stable periodic responses exist over a limited range of the external excitation frequency around the system's non-linear resonant frequency (the averaging method, or any other perturbation method, is effective only inside this range). Take $\beta = 0{\cdot}5$ for example, then $y_E = 0{\cdot}901$. The stable steady state periodic responses exist over Ω range of 0·87–1·36 and 0·44–1·55 for $k = 0{\cdot}5$ and 1 respectively. As $y_E \in [a, a + b]$, so the quasi-periodic motion occurs in the sliding stage. But if $\beta = 1$, then $y_E = 1{\cdot}38$, so the quasi-periodic motion occurs in constraint stage.

The results of numerical simulations are represented by "o" in Figure 5, which shows that for $\beta = 0{\cdot}5$, both the amplitudes of the steady state periodic responses and the frequency ranges over which the steady state periodic responses exist can be predicted very accurately. For $\beta = 1$, though the amplitudes are not as accurate as in the former case, the predicted frequency ranges can still be quite accurate.

5. MODE-LOCKING IN THE SELF-EXCITED SYSTEM WITH HYSTERETIC NON-LINEARITY

Dynamic systems in quasi-periodic motions can undergo mode-locking (or frequency, phase locking or entrainment) in which the two frequencies are related by a fixed ratio of

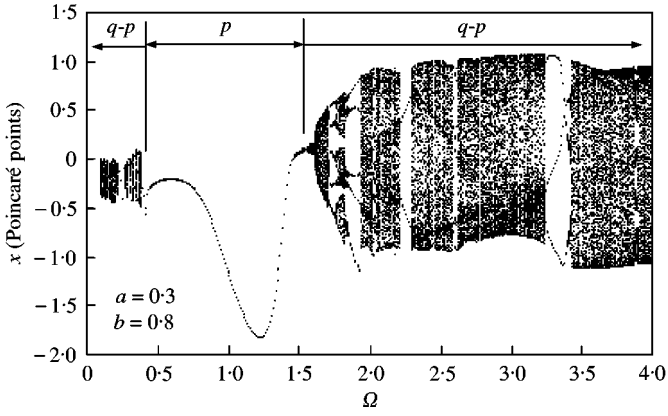

Figure 6. Bifurcation charts of the system ($a = 0{\cdot}3$, $b = 0{\cdot}8$, $\alpha = 1$, $\beta = 0{\cdot}5$ and $k = 1$): p, periodic motion; q-p, quasi-periodic motion.

integers p/q [11–13]. Circle maps have long been used to reveal the transitions from quasi-periodic regimes to chaos as well as quasi-periodic behaviour and mode-locking. By using circle maps, a so-called winding number $\rho = f_{cr}/f$, that is, the ratio of the non-linear resonant frequency to the forcing frequency can be obtained [14]. If ρ is irrational, the response of the system is quasi-periodic. The discrete points of the first order Poincaré map, obtained by sampling solutions of the system stroboscopically at $t = 0, 2\pi/\Omega, 2(2\pi/\Omega), \ldots$, wind around a closed curve. If ρ is rational, i.e., $\rho = p/q$, the response of the system is q-periodic, or in p/q mode-locking state. Then, q clusters of the first order Poincaré points wind around a closed curve, as a whole, with intervals. Selecting a suitable hyper plane in the state space which transverses the trajectory of the system as the second order Poincaré section, one finds p second order Poincaré points during the appearance of any successive q first order Poincaré points. This characteristic can be used to determine the rational winding number simply and efficiently.

From the definition of the winding number, it is found that $\rho > 1$ when the frequency of the external force is lower than the non-linear resonant frequency (i.e., $f < f_{cr}$); otherwise, $\rho < 1$ (i.e., $f > f_{cr}$). The p/q mode-locking states are also referred to as super- or subharmonic resonances of order p/q (p order superharmonic resonance for $q = 1$). Many studies suggest that the mode-locking states can remain, or the frequency ratio can be locked, over a finite range of one or another system parameter space, such as the forcing frequency. The winding number represents the order of mode-locking which could be organized according to the Farey tree, although some locking intervals are too narrow to be detected in actual numerical simulations or experimental studies [12].

Letting $a = 0{\cdot}3$, $b = 0{\cdot}8$, $\alpha = 1$, $\beta = 0{\cdot}5$ and $k = 1$, the bifurcation chart of the responses of the system (7) are obtained by numerical simulation over the forcing frequency Ω range of 0·1–4·0, i.e., including the primary resonance ($\Omega \approx 1$), as shown in Figure 6. As already mentioned, the primary periodic motion exists when $\Omega = 0{\cdot}44$–$1{\cdot}55$, and the motion outside this range should be quasi-periodic. The bifurcation chart proves the theoretically predicted result. The mode-locking alternates with quasi-periodic responses both before and after the primary resonance using circle maps. Some results are shown in Figure 7 in which the winding number ρs, phase portraits, first order Poincaré maps and spectra of x component are included. The superharmonic resonances with order up to 4 and subharmonic resonances with order up to $\frac{1}{3}$ are depicted. Figure 6 shows that it is easy to identify the various orders of subharmonic resonances due to the general fact that the locked ranges are

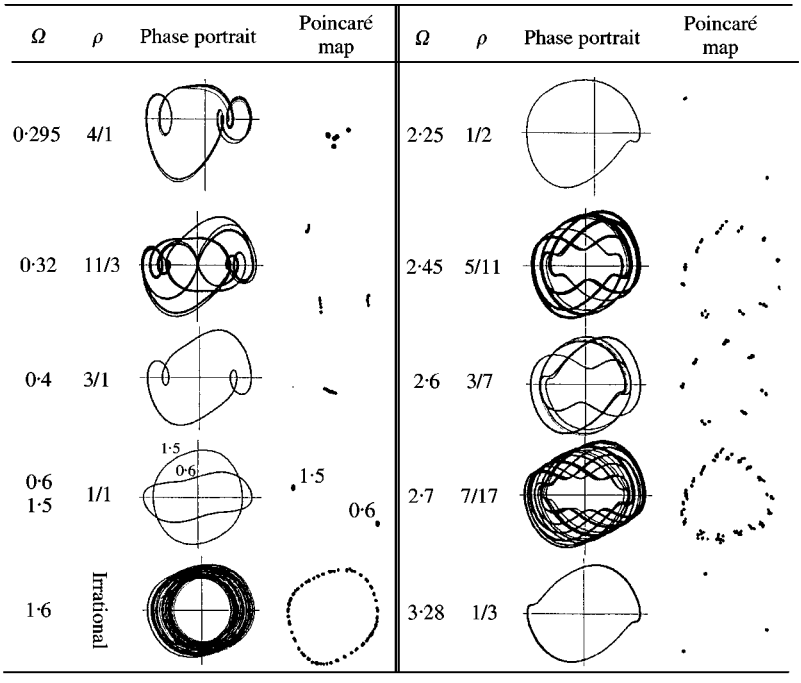

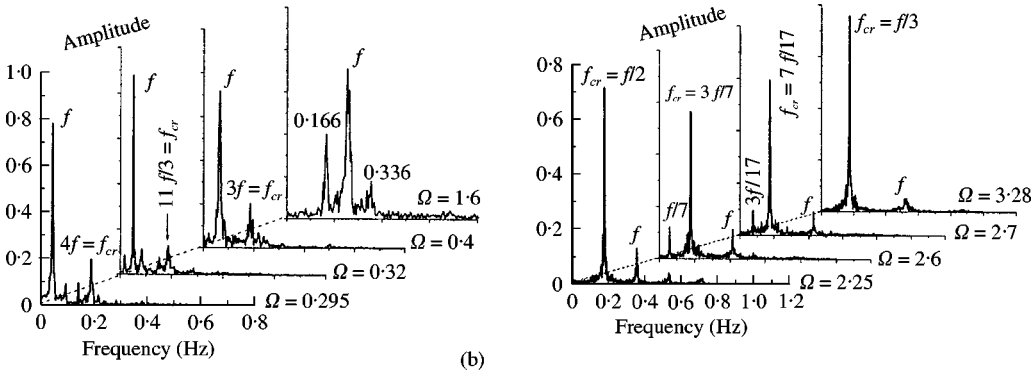

Figure 7. The mode-lockings alternating with quasi-periodic responses both before and after the primary resonance: (a) winding number ρs, phase portraits and Poincaré maps; (b) spectra of x component.

rather wide such as the states of $\rho = 4/5$ ($\Omega = 1{\cdot}71$–$1{\cdot}75$), $3/5$ ($\Omega = 1{\cdot}83$–$1{\cdot}92$), $3/7$ ($\Omega = 2{\cdot}58$–$2{\cdot}62$), $1/2$ ($\Omega = 2{\cdot}21$–$2{\cdot}28$) and $1/3$ ($\Omega = 3{\cdot}23$–$3{\cdot}4$). But the opposite situation is found through careful investigation when $a = 0{\cdot}2$ and $b = 0{\cdot}2$. The results suggest that the stronger the hysteresis effect (as the hysteretic parameters' values are increased), the more stable the subharmonic resonances. In the case of subharmonic resonances, the vibrations can be violent and bring the structures into danger [1].

The Farey number tree with $\frac{1}{2}$ and $\frac{1}{3}$ at the top level are shown in Figure 8. Under the guidance of the Farey number tree, the rational winding numbers between $\frac{1}{2}$ and $\frac{1}{3}$ can be identified as a function of Ω for $a = 0{\cdot}3$ and $b = 0{\cdot}8$, and the result is shown in Figure 9. Similar to many other published studies, though there are many obvious "steps" indicating the mode-locked ranges of Ω, there are still some cases predicted by the Farey tree, even in the third level from the top, that cannot be identified by simulation.

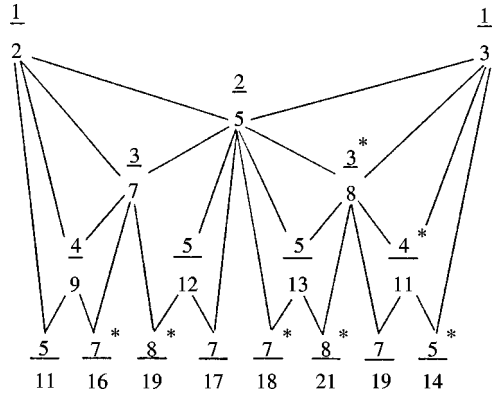

Figure 8. Mode-locking tongues positioned in a Farey number tree. Cases with superscript * were not identified in Figure 9.

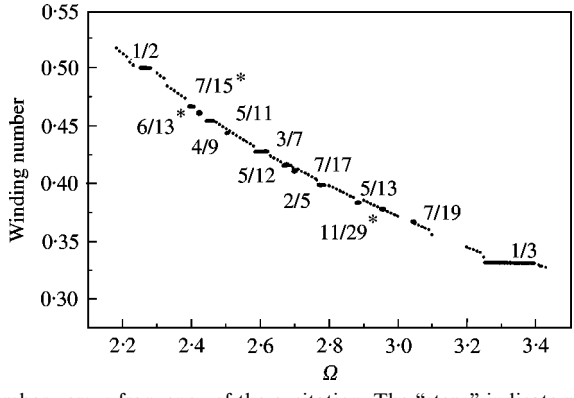

Figure 9. Winding number versus frequency of the excitation. The "steps" indicate mode-locking. Cases with superscript * belong to the lower level not shown in Figure 8.

The two frequencies f and f_{cr} are also referred to as fundamental in the sense that every peak in the spectra of the responses could be a linear combination of f and f_{cr}, such as $2f-f_{cr}$, $2f_{cr}-f$ or $f-2f_{cr}$, etc. For example, both $f/7$ for $\Omega = 2{\cdot}6$ and $3f/17$ for $\Omega = 2{\cdot}7$ in Figure 7 (b) are equal to $f-2f_{cr}$.

6. CONCLUSION

The non-linear dynamic behaviour of a van der Pol system with hysteretic non-linearity has been studied. The results showed that the first approximate analysis using the averaging method is quite adequate for determining the steady state responses of the system. The hysteretic non-linearity is found to display its effect on the steady state self-excited responses of the system mainly when the system is in the sliding stage, i.e., the Coulomb damper is always sliding when the mass changes its direction of motion. The response of the autonomous system can be multivalued and jumps can occur as the bifurcation parameter increases, whilst the non-autonomous system can exhibit softening spring behaviour in primary resonance. For the latter, further study revealed that the steady state response of the primary resonance loses its stability through Hopf bifurcation and then undergoes quasi-periodic motion as the frequency of the external force leaves a certain range. By using

circle maps to get the winding numbers, the super- and subharmonic resonances in various orders defined as mode-lockings were also investigated. The mode-lockings, alternating with quasi-periodic responses, take place according to the Farey number tree as has been revealed in many other systems. The increase of the hysteretic parameters' values to the conclusion that subharmonic resonances in various orders exist over a wider frequency range and can be identified more easily.

REFERENCES

1. A. H. NEYFEH and D. T. MOOK 1979 *Nonlinear Oscillations*, New York: John Wiley & Sons.
2. J. CARR 1981 *Application of Center Manifold Theory* New York: Springer-Verlag.
3. Y. S. CHEN and A. Y. T. LEUNG 1998 *Bifurcation and Chaos in Engineering*. London: Springer-Verlag.
4. P. R. SETHNA 1995 *Nonlinear Dynamics* **7**, 1–10. On averaged and normal form equations.
5. W. D. IWAN and D. M. FURUIKE 1973 *International Journal of Non-linear Mechanics* **8**, 395–409. The transient and steady-state response of a hereditary system.
6. E. H. DOWELL 1975 *Aeroelasticity of Plates and Shells*, Leyden: Noordhoff.
7. A. MUSZYNSKA 1986 *Journal of Sound and Vibration* **110**, 443–462. Whirl and whip: rotor/bearing stability problems.
8. Q. DING and J. E. COOPER 2000 *ISMA* 25, *International Conference on Noise and Vibration Engineering*, *Leuven*, *Belgium*, Paper XXII6. Hopf bifurcation analysis of a rotor/seal systems.
9. J. GUCKENHEIMER and P. HOLMES 1983 *Non-linear Oscillations*, *Dynamical Systems*, *and Bifurcations of Vector Fields*. New York: Springer-Verlag.
10. M. GOLUBITSKY and D. G. SCHAEFFER 1985 *Singularities and Groups in Bifurcation Theory*, Volume 1. New York: Springer-Verlag.
11. S. CHOI and S. T. NOAH 1994 *Journal of Applied Mechanics* **61**, 131–138. Mode-locking and chaos in a jeffcott rotor with bearing clearances.
12. H. HAUCKE and R. ECKE 1987 *Physica D* **25**, 307–329. Mode-locking and chaos in Rayleigh-Bénard convection.
13. H. J. KORSCH and H.-J. JODL 1994 *Chaos*: *A Program Collection for the PC*. Berlin: Springer-Verlag.
14. T. S. PARKER and L. O. CHUA 1989 *Practical Numerical Algorithms for Chaotic Systems*. New York: Springer-Verlag.